An Optimization-Based Approach

To

Injector Element Design

P. Kevin Tucker
NASA
Marshall Space Flight Center, AL 35812

Wei Shyy and Rajkumar Vaidyanathan
Department of Aerospace Engineering, Mechanics & Engineering Science
University of Florida
Gainesville, Florida 32611

ABSTRACT

An injector optimization methodology, *method i*, is used to investigate optimal design points for gaseous oxygen/gaseous hydrogen (GO$_2$/GH$_2$) injector elements. A swirl coaxial element and an unlike impinging element (a fuel-oxidizer-fuel triplet) are used to facilitate the study. The elements are optimized in terms of design variables such as fuel pressure drop, ΔP_f, oxidizer pressure drop, ΔP_o, combustor length, L_{comb}, and full cone swirl angle, Θ, (for the swirl element) or impingement half-angle, α, (for the impinging element) at a given mixture ratio and chamber pressure. Dependent variables such as energy release efficiency, *ERE*, wall heat flux, Q_w, injector heat flux, Q_{inj}, relative combustor weight, W_{rel}, and relative injector cost, C_{rel}, are calculated and then correlated with the design variables. An empirical design methodology is used to generate these responses for both element types. *Method i* is then used to generate response surfaces for each dependent variable for both types of elements. Desirability functions based on dependent variable constraints are created and used to facilitate development of composite response surfaces representing the five dependent variables in terms of the input variables. Three examples illustrating the utility and flexibility of *method i* are discussed in detail for each element type. First, joint response surfaces are constructed by sequentially adding dependent variables. Optimum designs are identified after addition of each variable and the effect each variable has on the element design is illustrated. This stepwise demonstration also highlights the importance of including variables such as weight and cost early in the design process. Secondly, using the composite response surface that includes all five dependent variables, unequal weights are assigned to emphasize certain variables relative to others. Here, *method i* is used to enable objective trade studies on design issues such as component life and thrust to weight ratio. Finally, combining results from both elements to simulate a trade study, thrust-to-weight trends are illustrated and examined in detail.

INTRODUCTION

In order to meet future launch program goals, the Spaceliner 100 Technology Roadmap[1] specifies very aggressive system goals for safety, life and cost per pound of payload launched into Earth orbit. Spaceliner 100 safety goals would decrease catastrophic events from the current 1 in 200 to 1 in 1,000,000 in 15 years. The life goal would be increased from the current 200 manned missions per year to 2000-5000 per year over the same time period. Concurrently, the cost goal aims to reduce the cost of delivering payloads to Earth orbit from the current $10,000 per pound to $1000 per pound in 10 years and to $100 per

* Aerospace Engineer, Member AIAA
† Professor, Dept. Chair., Associate Fellow AIAA
- Graduate Student Assistant, Student Member AIAA

pound in 15 years and ultimately to $10 per pound.

Design and development of advanced propulsion systems will be crucial to meeting these goals. Propulsion systems which meet these requirements must not only have high thrust to weight ratios, but also achieve higher operability and maintainability standards than in previous or current programs. Combustor designs, and injector designs in particular, will be key issues in meeting these goals. The injector design determines performance and stability, and is, therefore, the key factor governing injector face and chamber wall heat transfer/compatibility issues. Injector design also affects engine weight, cost, operability and maintainability.

The injector design methodologies used successfully in previous programs were typically based on large subscale databases and the empirical design tools derived from them[2,3,4,5,6]. These methodologies were often guided by extensive sub-and full-scale hot-fire test programs. Current and planned launch vehicle programs have relatively low budgets and aggressive schedules; neither of which is conducive to the large test programs of the past. New requirements for operability and maintainability require that the injector design be robust. Also, the goal for increased robustness will require evaluation of a larger design space earlier in the design process. Hence, development of broader and more efficient injector design methodologies seems to be a worthy pursuit.

This work demonstrates a new design methodology called *method i* [7,8](Methodology for Optimizing the Design of Injectors) which seeks to address the above issues in the context of injector design. Simply put, *method i* is used to generate appropriate design data and then guide the designer through the information toward an optimum design subject to his specified constraints. Since *method i* is structured so that any pertinent information source can be used, design data can be obtained from existing databases and empirical design methodologies. If required, new data can be generated with modern experimental techniques or appropriate CFD models.

As implied above, *method i* is comprised of two discrete entities. The first element is the tool used to generate the design data—in this work, an empirical design methodology for GO_2/GH_2 injectors generated by Calhoon et al.[9,10] The second element in *method i* is a group of optimization techniques. It is the optimization capability that extends *method i* beyond previous injector design methodologies. The optimization scheme allows large amounts of inter-related information to be managed in such a way that the extent to which variables influence each other can be objectively evaluated and optimal design points can be identified and evaluated with confidence. In this work, the Response Surface Method (RSM)[11] is used to facilitate the optimization. The RSM approach is to conduct a series of well-chosen experiments (i.e., numerical, physical, or both) and use the resulting function values to construct a global approximation (i.e., response surface) of the measured quantity (i.e., response) over the design space. A standard constrained optimization algorithm is then used to interrogate the response surface for an optimum design.

The approach used to develop and demonstrate this new methodology is divided into three main tasks. Task 1 is a proof of concept where the basic methodology is developed and demonstrated on single element injectors. Work on Task 1 for the shear coaxial element has been reported previously.[7,8] The work for the swirl coaxial and impinging elements, which completes the empirical database for Task 1, is presented below. To conclude Task 1, all the design data, along with optimization techniques developed to date, will be demonstrated in an element selection/preliminary design process.

Task 2 involves replacing/augmenting the empirical data with data from physical and numerical experiments (i.e., test data and validated CFD analyses). Task 3 involves using CFD analyses and empirical methods to design a multi-element injector consisting of 7-12 elements. Optimization will be done in the context of single element variables plus element pattern, element spacing, film cooling, etc.

SCOPE OF CURRENT EFFORT

This paper presents the design optimization of both a swirl coaxial injector element and a fuel-oxidizer-fuel (F-O-F) impinging injector element. The swirl coaxial element has been used somewhat sparingly in this country, but has been widely used in Russia because of its reported ability to perform well over a large throttle range.[12] A schematic of the element is shown in Fig. 1. The empirical design

methodology of Calhoon et al uses the oxidizer pressure drop, ΔP_o, fuel pressure drop, ΔP_f, combustor length, L_{comb}, and the full cone swirl angle, Θ, as independent variables. Due to stability considerations for this injector design, the ΔP_o range is set to 10-20% of the chamber pressure, while the ΔP_f range is set to 2-20% of chamber pressure. The combustor length, defined as the distance from the injector to the end of the

barrel portion of the chamber ranges from 2-8 inches. The full cone swirl angle is allowed to vary from 30-90°. The dependent variables modeled are ERE (a measure of element performance), wall heat flux, Q_w, injector heat flux, Q_{inj}, relative combustor weight, W_{rel}, and relative injector cost, C_{rel}.
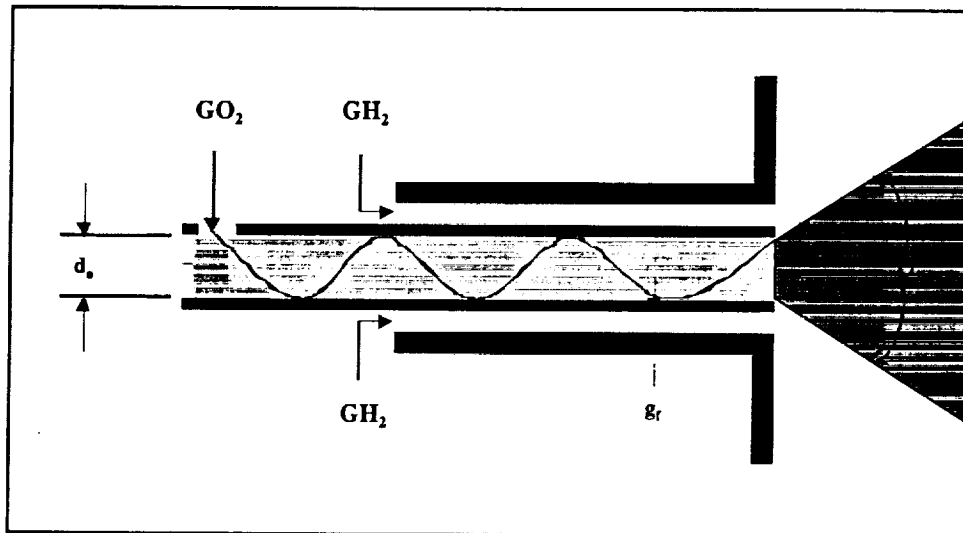
Figure 1. Swirl Coaxial Injector Element Schematic

The F-O-F triplet element type is widely used and is capable of operating at high efficiency levels. A schematic of an F-O-F element is shown in Fig. 2. The empirical design methodology of Calhoon et al uses the oxidizer pressure drop, ΔP_o, fuel pressure drop, ΔP_f, combustor length, L_{comb}, and the impingement half-angle, α as independent variables. For this injector design, the pressure drop range is set to 10-20% of the chamber pressure due to stability considerations. The combustor length again ranges from 2-8 inches. The impingement half angle is allow to vary from 15-50°. Dependent variables are, again, ERE, wall heat flux, Q_w, injector heat flux, Q_{inj}, relative combustor weight, W_{rel}, and relative injector cost, C_{rel}.
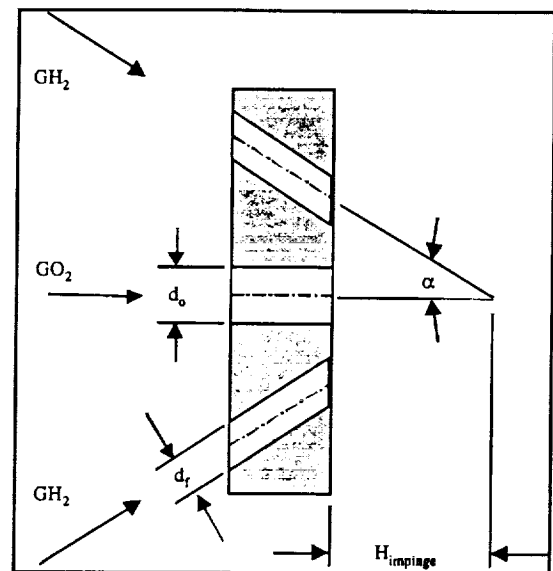
Figure 2. Schematic of F-O-F Injector Element

In the following sections, the injector models and the generation of design data are briefly discussed. Response surfaces for each of the dependent variables are generated and then combined into a joint surface for each element to facilitate the optimization process. Optimization of each element is demonstrated by applying equal weights for all dependent variables as they are added to the joint response surface one at a time and, then, by applying unequal weights that might reflect specific design priorities and trades. Finally, thrust-to-weight ratio trends are for each element are examined and compared.

INJECTOR DESIGN MODELS
This section provides details of the models used to generate the design data for the dependent variables previously noted.

SWIRL COAXIAL ELEMENT DESIGN MODEL
The process for generating the design data for the swirl coaxial element is described and sample results are also presented. The chamber pressure, mixture ratio, and propellant flow rates selected for this example are:

$$P_c = 1000 psi$$
$$MR = 6$$
$$m_{GO_2} = 0.25 lb_m / sec$$
$$m_{GH_2} = 0.042 lb_m \ sec$$

The gaseous propellants are injected at a temperature of 540 R.

Dependent Variable Models
Reference to Figure 1 shows that the GO_2, flowing in the center post of the element, exits the element with both radial and axial velocity components. This effect is achieved by introducing the GO_2 tangentially into the center post through small slots. When the GO_2, under hydrostatic head, is forced through the tangential slots, part of the pressure head is converted into a velocity head, causing a rotational velocity in the element. With the operating conditions fixed at the above-noted levels, the work of Doumas and Laster[13] is used to define the element geometry required to generate GO_2 swirl angles. Although developed for liquids, this work has been used

successfully to design swirl coaxial elements for gaseous propellants.[14,15] For a specified ΔP_o and swirl angle, Θ, the number and size of tangential slots, the discharge coefficient, the GO_2 center post diameter, d_o, and the radial and axial GO_2 velocity components, V_{or} and V_{oa} are calculated. These quantities are then used to determine the dependent variables for each design condition.

The element ERE, calculated according to the empirical design methodology of Calhoon et al., is a function of all four independent variables noted above. A cold flow mixing efficiency, $E_{m,90}$, for $\Theta = 90°$, is correlated by:

$$E_{m,90} = 100 - 5 \ln \left[\frac{K_s}{L_{cold}/d_o} \right] \quad (1)$$

The cold flow mixing length, L_{cold}, is correlated from a known chamber length, L_{comb}. The GO_2 post diameter, d_o, is a function of ΔP_o and Θ. Smaller values of d_o correspond to large values of ΔP_o and smaller swirl angles. The empirical swirl factor, K_s, is a function of the normalized differential injection velocity, $(V_f-V_o)/V_o$. K_s increases with increasing normalized differential injection velocity for the range of propellant velocities considered in this effort. For fixed propellant mass flow rates, the velocities V_o and V_f are functions of their pressure drops across the injector, ΔP_o and ΔP_f, respectively. For a given ΔP_o, V_o also depends on the swirl angle. Lower V_o's are a product of higher swirl angles. Cold flow mixing is thereby enhanced with higher values of V_o (i.e. ΔP_o) and L_{comb}. Lower values of V_f (i.e. ΔP_f) and Θ also tend to enhance cold flow mixing.

A fractional factor, f_s, is applied to $E_{m,90}$ to account for the lower levels of cold flow mixing found with swirl angles less than 90°. The resultant measure of cold flow mixing, $E_{m,\Theta}$, is a product of $E_{m,90}$ and f_s. This factor, for a given design, is a function of the normalized differential injection velocity and the ratio of radial to axial GO_2 velocity, V_{or}/V_{oa}. Increasing values of both quantities increase f_s, with a value of $f_s = 1$ being found at $V_{or}/V_{oa} = 1$ ($\Theta = 90°$) for all values of $(V_f - V_o)/V_o$. Larger values of f_s increase cold flow mixing. These values are found at low ΔP_o and high ΔP_f and Θ. There is no dependency of f_s on chamber length. These trends are opposite those noted above. The effect of the competing influences of the independent

4

variables on *ERE* trends will be discussed later. Finally, *ERE* is proportional to $E_{m,\Theta}$.

The wall heat flux Q_w, is correlated with the propellant momentum ratio as defined by:

$$MR = \frac{m_o u_o}{m_f u_f} \qquad (2)$$

The wall heat flux curve from the Calhoon et al. methodology is fairly flat, varying only about 10% from high to low for the range of pressure drops considered in this effort. Q_w decreases with increasing V_o (high ΔP_o and low Θ) and decreasing V_f (low ΔP_f). That Q_w would decrease with increasing V_o is counter to intuition. It seems that high values of V_o, for any Θ, would result in higher mixture ratios in the wall region as is the case for liquid O_2. This effect is not discussed by Calhoon et al. The CFD analysis to be done in Task 2 should clarify this situation. For this effort, the model for Q_w is used as is.

The heat flux seen by the injector, Q_{inj}, is actually modeled by the distance from the injector at which the propellant streams intersect. This axial distance is measured at the radial position corresponding to the center of the coaxial fuel annulus, or gap. It is here that the streams begin to mix and burn. This measure is qualitative, but captures the trend that higher injector heat fluxes occur the nearer the injector that the combustion begins. The axial distance is affected directly by the swirl angle, and, indirectly, by the propellant pressure drops. Q_{inj} decreases with decreasing swirl angle, increasing GO_2 pressure drop and decreasing GH_2 pressure drop. Swirl angle has the largest effect, while ΔP_o is the least significant factor.

The relative combustor weight, W_{rel}, is simply a function of the combustor length, L_{comb}, the distance from the injector to the end of the barrel portion of the chamber. The longer the combustor, the more it weighs.

The relative injector cost, C_{rel}, is a function of the fuel gap width and the width of the tangential slots used to induce the swirl in the GO_2 center post. Larger values of both variables result in lower machining costs, and thus lead to lower injector cost. The fuel gap width increases with increasing ΔP_o, and decreasing values of ΔP_f and Θ. Swirl slot width increases with lower values of ΔP_o and Θ. Overall, C_{rel} decreases with increasing ΔP_o and decreasing ΔP_f and Θ. Fuel

pressure drop and swirl angle are the most significant factors.

Generation of Design Data

The operating conditions given above and the noted independent variables (constrained to the previously noted ranges) are used to generate the design data for element optimization studies. A matrix of propellant pressure drop combinations was developed and nine combinations were selected for use in populating the design data base. There are 20 combinations of L_{comb} and Θ for each ΔP combination, making a total of 180 design points selected.

F-O-F INJECTOR MODEL

The process for generating the design data for the F-O-F impinging element is described and sample results are also presented. The conditions selected for this example are the same as for the swirl coaxial element:

$$P_c = 1000\,psi$$
$$MR = 6$$
$$m_{GO_2} = 0.25\,lb_m / sec$$
$$m_{GH_2} = 0.042\,lb_m\,sec$$

The gaseous propellants are injected at a temperature of 540 R.

Dependent Variable Models

Again, the empirical design methodology of Calhoon et al is used to characterize the *ERE* and Q_w. For *ERE*, a cold flow mixing efficiency is correlated by

$$E_m = 100 - K_T \ln\left[\frac{9.5}{L_{cold}/d_o}\right] \qquad (3)$$

The cold flow mixing length, L_{cold}, is correlated from a known chamber length, L_{comb}. The GO_2 orifice diameter, d_o, is a function of ΔPo. For the impinging element, the methodology uses a quantity called the normalized injection momentum ratio, MR_{ni}, to correlate the mixing at the different design points. Here

$$K_T = f(MR_{ni}) \qquad (4)$$

where

$$MR_{ni} = \frac{2.3 m_o u_o}{m_f u_f \sin \alpha} \quad (5)$$

The minimum K_T, and thus maximum mixing and ERE, occurs at an MR_{ni} of 2.0. Since the propellant mass flowrates are fixed, only the propellant velocities and the impingement half-angle influence the normalized injection momentum ratio. The velocities are proportional to the square root of the respective pressure drops across the injector, ΔP_o and ΔP_f. For the flow conditions and variable ranges considered in this problem, MR_{ni} ranges from 3.2 to 17.8. Accordingly, lowering ΔP_o, raising ΔP_f, increasing α, or some combination of these actions tend to increase ERE.

The wall heat flux is again correlated with the propellant momentum ratio as defined by

$$MR = \frac{m_o u_o}{m_f u_f} \quad (6)$$

For the F-O-F triplet element, the maximum wall heat flux occurs at a momentum ratio of approximately 0.4. High heat flux is the result of over-penetration of the fuel jet which produces a high O/F in the wall region. For the flow conditions and variable ranges considered in this effort, MR ranges from 1.06 to 2.11. Hence, increasing the value of this ratio by either increasing ΔP_o or decreasing ΔP_f lowers the wall heat flux.

The heat flux seen by the injector face, Q_{inj}, is qualitatively modeled by the impingement height, $H_{impinge}$. The notion being that, as the impingement height decreases, the combustion occurs closer to the injector face, causing a proportional increase in Q_{inj}. Thus, for the purposes of this exercise, Q_{inj} is modeled as the reciprocal of the $H_{impinge}$. Impingement height is a function of α and ΔP_f. Reference to Fig. 2 shows that as α is increased, $H_{impinge}$ is shortened. The dependence of $H_{impinge}$ on the fuel orifice diameter, d_f, and thus, ΔP_f, results from making the freestream length of the fuel jet, L_{fs}, a function of d_f[16]. For each ΔP_f, L_{fs} was set to six times d_f for an impingement half-angle of $30°$. So, as d_f increases (corresponding to decreasing ΔP_f), L_{fs} increases, as does $H_{impinge}$.

The models for W_{rel} and C_{rel} are simple but represent the correct trends. W_{rel} is a function only of L_{comb}, the combustor length from injector face to the end of the chamber barrel section. The dimensions of the rest of the thrust chamber assembly are assumed to be fixed. So, as L_{comb} increases, W_{rel} increases accordingly. The model for C_{rel} is based on the notion that smaller orifices are more expensive to machine. Therefore, C_{rel} is a function of both propellant pressure drops. As the ΔP's increase, the propellant velocity through the injector increases and the orifice area decreases. So, as either, or both, ΔP_o and ΔP_f increase, C_{rel} increases.

Generation of Design Data
The system variables given above and independent variables (constrained to the previously noted ranges) are used to generate the design data for element optimization studies. Since propellant momentum ratio is an important variable in the empirical design methodology, a matrix of momentum ratios was developed over the 100-200 psi propellant pressure drop range. Nine pressure drop combinations were selected for use in populating the design data base. There are 20 combinations of L_{comb} and α for each ΔP combination, making a total of 180 design points selected.

RESPONSE SURFACE GENERATION
In this effort, $method$ i uses the Response Surface Method (RSM) to find optimal values of ERE, Q_w, Q_{inj}, W_{rel} and C_{rel} for acceptable values of ΔP_o, ΔP_f, L_{comb} and Θ or α. The approach of RSM is to perform a series of experiments, or numerical analyses, for a prescribed set of design points, and to construct a response surface of the measured quantity over the design space. In the present context, the five responses of interest are ERE, Q_w, Q_{inj}, W_{rel} and C_{rel}. The design space for each element consists of the set of relevant design variables ΔP_o, ΔP_f, L_{comb} and Θ or α. The response surfaces are fit by standard least-squares regression with a quadratic polynomial using the JMP[17] statistical analysis software. JMP is an interactive, spreadsheet-based program which provides a variety of statistical analysis functions. A backward elimination procedure based on t-statistics is used to discard terms and improve the prediction accuracy[18].

6

When the JMP software is used to analyze the 180 design points, five individual full response surfaces for the variables in the design space are approximated by quadratic polynomials that contain 15 terms each.

In the current study, it is desirable to attempt to maximize ERE and while simultaneously minimizing Q_w, Q_{inj}, W_{rel} and C_{rel}. One method of optimizing multiple responses simultaneously is to build from the individual responses a composite response known as the desirability function. The method allows for a designer's own priorities for the response values to be built into the optimization procedure. The first step in the method is to develop a desirability, d, for each response. In the case where a response should be maximized, such as ERE, the desirability takes the form:

$$d_1 = \left(\frac{ERE - A}{B - A}\right)^s \qquad (7)$$

where B is the target value and A is the lowest acceptable value such that $d = 1$ for any $ERE > B$ and $d = 0$ for $ERE < A$. The power value s is set according to one's subjective impression about the role of the response in the total desirability of the product. In the case where a response is to be minimized, such as Q_w, the desirability takes on the form:

$$d_2 = \left(\frac{Q - E}{C - E}\right)^t \qquad (8)$$

where C is the target value and E is the highest acceptable value such that $d = 1$ for any $Q_w < C$ and $d = 0$ for $Q_w > E$. Choices for A, B, C, and E are chosen according to the designer's priorities or, as in the present study, simply as the boundary values of the domain of ERE and Q_w .

Choices for s and t are more difficult, but plots such as Figure 2 can be instructive. Figure 3 shows the appearance of the desirability function for the case of maximizing a response. Desirabilities with $s << 1$ imply that a product need not be close to the response target value, B, to be quite acceptable. But $s = 8$, say, implies that the product is nearly unacceptable unless the response is close to B.

A single composite response is developed which is the geometric mean of the desirabilities of the
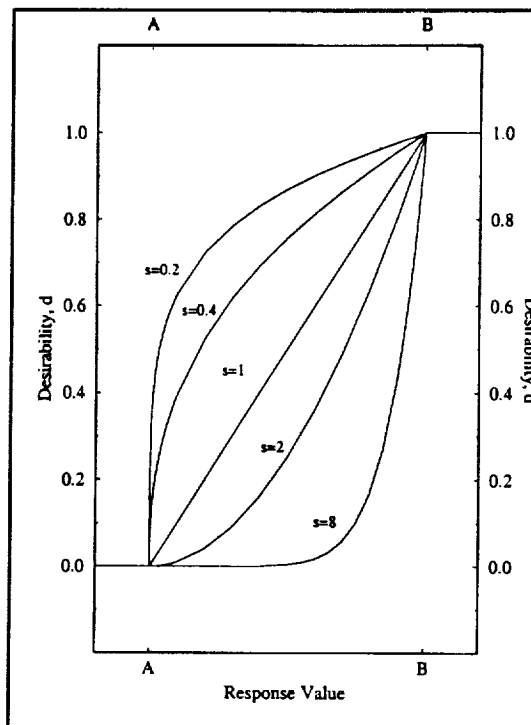
Figure 3. Desirability Function for Various Weight Factors, s.

individual responses. The composite response is defined as:

$$D = \left(d_1 \cdot d_2 \cdot d_3 .... d_m\right)^{1/m} \qquad (9)$$

The complete joint response surface for the present study is given by:

$$D = \left(d_{ERE} d_{Q_w} d_{Q_{inj}} d_{W_{rel}} d_{C_{rel}}\right)^{1/5} \qquad (10)$$

OPTIMIZATION RESULTS AND DISCUSSION

Results are presented for each element in two parts. The first set of results for each element are obtained by building the joint response surface with the addition of one dependent variable at a time. The second set of results for each element illustrate an emphasis on performance and life issues. Finally, results for the two element are combined to compare the thrust-to-weight ratio trends for the different element types.

SWIRL COAXIAL ELEMENT

Two sets of results are presented below to demonstrate the capability and flexibility of *method i* for the swirl coaxial injector element design. These examples illustrate the effect of each variable on the optimum design and the trade-offs between life and performance issues.

Effect Of Each Variable On Element Design

The results in this section were obtained by building the joint response surface with the addition of one dependent variable at a time. The results are shown in Table 1. Case 1 seeks the maximum performance without regard to the effect on the other dependent variables. *ERE* is a fairly strong function of L_{comb}—longer chamber lengths allow more residence time for the propellant to mix and burn. The effect of Θ on *ERE* is strongest at low values of Θ. *ERE* increases with increasing Θ until about $\Theta = 80°$ and then fall off slightly due to the competing influences noted earlier. These competing influences also cause the effect of both pressure drops on ERE to be somewhat flat, although since ΔP_o affects more variables, its influence is slightly stronger. Maximum performance is found at high values of ΔP_o, Θ, and L_{comb} and at low values of ΔP_f. This trend is consistent with other works for similar injector elements.[14,15] The value of 98.5 found by the optimizer is indeed the highest predicted by this model. However, since the model developed by Calhoon et al. has been shown to slightly under-predict swirl coaxial element performance, the actual value is likely somewhat higher.

The objective of Case 2 is to simultaneously maximize ERE and the minimize Q_w. Table 2 shows that the exact same design point was chosen as for Case 1. Usually, the design which yields the maximum ERE also produces a high wall heat flux. That is not the case here; this issue has already been noted. The minimum Q_w is found in the region of high ΔP_o and low ΔP_f. In this area, Q_w is almost independent of Θ. Hence, the minimum Q_w can still be found a the high value of Θ required to maximize ERE. It should be noted that in the low ΔP_o, high ΔP_f region, Q_w is a function of Θ. Here, as Θ is increased, Q_w increases since the larger swirl angle forces d_o to increase and thus decrease V_o. In the Calhoon et al. model, this reduction in GO_2 momentum causes an increase in Q_w.

The requirement to minimize Q_{inj} is added in Case 3. In order to minimize Q_{inj}, the swirl angle is decreased from 81° to 37°, thus reducing the injector face heat flux by approximately a factor of 3. This decrease in Θ also lowers *ERE* which forces use of a longer chamber to offset some of the loss. Still, *ERE* is reduced by over one percent.

Case 4 considers the desire to minimize the chamber weight, W_{rel}, in addition to maximizing *ERE* and minimizing Q_w and Q_{inj}. Since W_{rel} depends only on L_{comb}, the chamber length is shortened by over half. The weight is reduced, but so is *ERE*. To mitigate the adverse effect on *ERE*, Θ is increased by almost 10°,. simultaneously increasing Q_{inj}. *ERE* drops again by over a percent, while Q_w remains constant.

Independent Variable	Constraints	Results Case 1	Results Case 2	Results Case 3	Results Case 4	Results Case 5
ΔP_o	100-200	200	200	200	200	104
ΔP_f	20-200	41	41	42	47	20
L_{comb}	2-8	7.2	7.2	7.6	3.2	3.4
Θ	30-90	81	81	37	47	44
Dependent Variable	Desirability Limits	ERE	ERE & Q_w	ERE, Q_w, Q_{inj}	ERE, Q_w, Q_{inj}, W_{rel}	ERE, Q_w, Q_{inj}, W_{rel}, C_{rel}
ERE	92.3-99.0	98.5	98.5	97.2	96.0	95.7
Q_w	0.596-0.647	0.596	0.596	0.596	0.596	0.596
Q_{inj}	6.95-36.59	26.8	26.8	9.1	12.0	10.5
W_{rel}	0.900-1.154	1.13	1.13	1.14	0.97	0.98
C_{rel}	0.73-1.42	0.98	0.98	0.81	0.84	0.76

Table 1. Effect of Each Variable on the Design-Optimal Designs for Original Constraints and Equal Weights for Swirl Coaxial Element.

Finally, minimizing the injector cost, C_{rel}, is added in Case 5. The relative injector cost is lowered by decreasing each pressure drop approximately a factor of 2. Decreasing ΔP_f results in a larger fuel gap and decreasing ΔP_o allows for a larger swirl slot. These factors combine to lower the cost by almost 10 %.

Although several of the variables included in this exercise are qualitative, an important conclusion can still be drawn. The sequential addition of dependent variables to an existing design results in changes to independent and dependent variables in the existing design. The direction and magnitude of these changes depends on the sensitivity of the variables, but the changes may well be significant. The design in Case 5 is quite different that the one in Case 1. Consideration of a larger design space results in a different design—the sooner the additional variables are considered, the more robust the final design.

Emphasis on Life and Performance Issues

The purpose of this section is to illustrate the effect of emphasizing certain aspects of the design during the optimization process. *Method i* allows this emphasis via the weights applied to the desirability functions in the joint response surface. The set of results shown in Table 2 facilitate the illustration. The baseline results in Table 2 (repeated from Case 5 in Table 1) consider the entire design space using the original constraints and equal weights for the dependent variables. The results in for Case 1 are obtained by emphasizing the minimization of the

wall and injector face heat fluxes. Desirability functions for both of these variables are given lower heat fluxes tend to increase component life, weighting these two variables is equivalent to emphasizing a life-type issue in the design. Since Q_w is already at its minimum value, it remains fixed. As expected, Θs decreased which decreases the value of Q_{inj} by almost 35%. The lower value of Θ also produces a lower ERE. Both propellant pressure drops and the combustor length are increased to mitigate the drop in ERE. The increases in L_{comb} and ΔP_f cause increases in W_{rel} and C_{rel}, respectively. The emphasis on life extracts the expected penalty on performance. Additionally, for the swirl coaxial element model, there are also slight weight and cost penalties.

The results for Case 2 are obtained by emphasizing maximization of ERE and minimization of W_{rel} with desirability weightings of 10 and 5, respectively. Increased weighting for these two variables is equivalent to emphasizing a thrust to weight goal for the injector/chamber. The relative chamber length is shortened to slightly lower W_{rel}. ERE is maximized by increasing the GO_2 swirl angle by a factor of almost 2.5 and also increasing ΔP_f by over 35 %. The value of ERE rises by over one percent. As noted earlier, increasing Θ leads to increased injector heat flux. For this case, emphasis on thrust and weight tends to have an adverse affect on Q_{inj}. Relative cost for the swirl coaxial element model is also increased significantly.

Independent Variable	Constraints	Results Baseline	Constraints	Results Case 1	Constraints	Results Case 2
ΔP_o	100-200	104	100-200	200	100-200	200
ΔP_f	20-200	20	20-200	32	20-200	44
L_{comb}	2-8	3.4	2-8	3.6	2-8	2.9
Θ	30-90	44.0	30-90	30.0	30-90	72.0
Dependent Variable	Baseline Variable Weight		Life Variable Weight		Thrust/Weight Variable Weight	
ERE	1	95.7	1	95.3	10	96.7
Q_w	1	0.596	5	0.596	1	0.596
Q_{π}	1	10.5	10	6.9	1	22.6
W_{rel}	1	0.98	1	0.99	2	0.96
C_{rel}	1	0.76	1	0.79	1	0.94

Table 2. Effect of Emphasizing Life and Performance Issues for the Swirl Coaxial Element.

IMPINGING ELEMENT

Two sets of results are presented below to demonstrate the capability of *method i* for the impinging injector element design. These two examples illustrate the effect of each variable on the optimum design and the trade-offs between life and performance issues.

Effect Of Each Variable On Element Design

The results in this section were obtained by building the joint response surface with the addition of one dependent variable at a time. The results are shown in Table 3. Since current non-optimizer based design methods yield high-performing injector elements, simply maximizing the ERE is not a challenge. Accordingly, the initial results (Case 1) are obtained with a joint ERE and Q_w response surface. The results in Case 2 have the impingement height added, Case 3 adds the relative chamber weight and the relative cost is added in Case 4. All results are obtained using the original independent variable constraints and all dependent variables have equal weights of one. The results for Case 1 show that ERE is at its maximum and Q_w is very near its minimum desirability limit. Minimizing Q_w requires a small ΔP_f relative to ΔP_o as evidenced by the values of 100 psi and 183 psi, respectively. Maximum ERE values are found at the longest chamber length, $L_{comb}=8$ inches. Even with the relatively high value of 183 psi for ΔP_o and low value of ΔP_f of 100 psi, ERE is maximized to 99.9% with an impingement half-angle of 33.1°.

Addition of the impingement height to Case 2 to model the injector face heat flux, Q_{inj}, forces α lower to increase $H_{impinge}$ and decrease Q_{inj}. This decrease in the radial component of the fuel momentum has an adverse affect on ERE. This effect is mitigated to a degree by increasing the ΔP_f by 32 psi to 132 psi. ERE is still reduced by 1.6%. Also, the increase in ΔP_f causes increased penetration of the fuel jet which results in a slightly higher Q_w.

Case 3 adds the relative combustor weight to the list of dependent variables modeled. Since W_{rel} is only a function of L_{comb}, minimizing W_{rel} shortens the combustor length from 8 to 6.6 inches. The shorter L_{comb} tends to lower ERE. This effect is offset to a large degree by increases in ΔP_f and α, both of which increase the radial component of the fuel momentum. The increase in ΔP_f also causes a slight increase in Q_w. The increase in α causes a significant decrease in $H_{impinge}$ which increases the injector face heat flux.

Finally, the relative cost of the injector is added in Case 5. Since C_{rel} is only a function of propellant pressure drops, both ΔP_o and ΔP_f are driven to their respective minimum values. This and a slight increase in α allow ERE to be maintained at 98%, even with a slight decrease in L_{comb}. The largest effect of this fairly dramatic decrease in propellant pressure drops is on Q_w. Even though the values for ΔP_o and ΔP_f fell, ΔP_f increased relative to ΔP_o causing Q_w to increase by almost 9%. Impingement height and relative combustor weight are essentially unchanged.

Independent Variable	Constraints	Results Case 1	Results Case 2	Results Case 3	Results Case 4
ΔP_o	100-200	183	183	179	100
ΔP_f	100-200	100	132	149	100
L_{comb}	2-8	8.0	8.0	6.6	6.5
α	15-50	33.1	18.9	22.3	24.0
Dependent Variable	Desirability Limits	ERE & Q_w	ERE, Q_w, $H_{impinge}$	ERE, Q_w, $H_{impinge}$, W_{rel}	ERE, Q_w, $H_{impinge}$, W_{rel}, C_{rel}
ERE	95.0-99.9	99.9	98.3	98.0	98.0
Q_w	0.7-1.3	0.74	0.76	0.79	0.86
$H_{impinge}$	0.2-1.0	0.40	0.75	0.61	0.63
W_{rel}	0.9-1.2	1.15	1.15	1.10	1.10
C_{rel}	0.7-1.1	0.98	1.00	1.01	0.93

Table 3. Effect of Each Variable on the Design--Optimal Designs for Original Constraints & Equal Weights for the Impinging Element.

The design in Case 4 is quite different that the one in Case 1. Again, consideration of a larger design space results in a different design—the sooner the additional variables are considered, the more robust the final design.

Emphasis on Life and Performance Issues

The purpose of this section is to illustrate the effect of emphasizing certain aspects of the design during the optimization process. *Method i* allows this emphasis via the weights applied to the desirability functions in the joint response surface. The set of results shown in Table 4 facilitate the illustration. The Case 1 (baseline) results are repeated from Case 4 in Table 3 where the entire design space is considered with the original constraints and equal weights for the dependent variables. The results in the Case 2 column are obtained by emphasizing the minimization of the wall and injector face heat fluxes. Desirability functions for both of these variables are given a weight of five. Since lower heat fluxes tend to increase component life, weighting these two variables is equivalent to emphasizing a life-type issue in the design. As expected, α is decreased to increase $H_{impinge}$, thus decreasing Q_{inj}. Since the fuel pressure drop is already at the minimum, the oxidizer pressure drop is increased by 58% to decrease Q_w. Both of these changes tend to decrease ERE. While ERE does decrease, the effect is somewhat mitigated by an increase in L_{comb}. The increases in L_{comb} and ΔP_o cause increases in W_{rel} and C_{rel},

respectively. Again, the emphasis on life imposes a penalty on performance. As with the swirl coaxial element, there are also weight and cost penalties for the impinging element.

The results for Case 3 are obtained by emphasizing maximization of ERE and minimization of W_{rel} with desirability weightings of five. Increased weighting for these two variables is equivalent to emphasizing a thrust to weight goal for the injector/chamber. The relative chamber length is shortened to lower W_{rel}. ERE is maximized by increasing the radial momentum of the fuel jet. Both ΔP_f and α are increased to accomplish ERE maximization. As noted earlier, increasing ΔP_f and α lead to increased wall and injector heat fluxes, respectively. Reference to Table 4 indicates that to be the case here. For this case, emphasis on thrust and weight tend to have an adverse affect on both Q_w and Q_{inj}. Relative cost, for the impinging element model, is not significantly affected.

THRUST TO WEIGHT RATIO TREND COMPARISONS

Results from both injector elements have been normalized to illustrate an emphasis on high thrust-to-weight designs. The results are shown in Figures 4 and 5. In Figure 4, the results of simultaneously increasing the weighting factors to increase ERE and decrease W_{rel} are shown. Although the impinging element has a higher ERE, the W_{rel} is also higher. With a slightly

Independent Variable	Constraints	Results Case 1	Constraints	Results Case 2	Constraints	Results Case 3
ΔP_o	100-200	100	100-200	158	100-200	100
ΔP_f	100-200	100	100-200	100	100-200	137
L_{comb}	2-8	6.5	2-8	7.7	2-8	5.2
α	15-50	24.0	15-50	15.0	15-50	36.0
Dependent Variable	Baseline Variable Weight		Life Variable Weight		Thrust/Weight Variable Weight	
ERE	1	98.0	1	96.7	5	99.1
Q_w	1	0.86	5	0.75	1	0.95
$H_{impinge}$	1	0.63	5	0.94	1	0.32
W_{rel}	1	1.10	1	1.14	5	1.05
C_{rel}	1	0.93	1	0.97	1	0.95

Table 4. Effect of Emphasizing & Life & Performance Issues—Optimal Designs for Original Constraints and Modified Weights for the Impinging Element.

lower *ERE* but significantly lower W_{rel}, the swirl element has the higher thrust-to-weight ratio. However, as weight minimization is emphasized, the impinging element weight continues to decrease after the swirl element weight has become constant. This indicates there is more room for improvement in thrust-to-weight ratio for the impinging element than the swirl element.
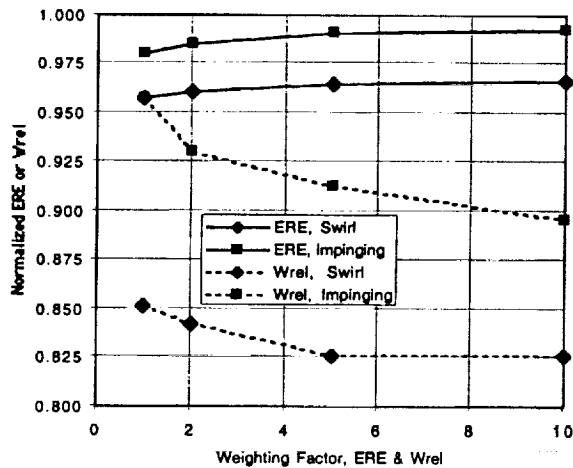
Figure 4. Performance and weight trends for swirl and impinging elements.
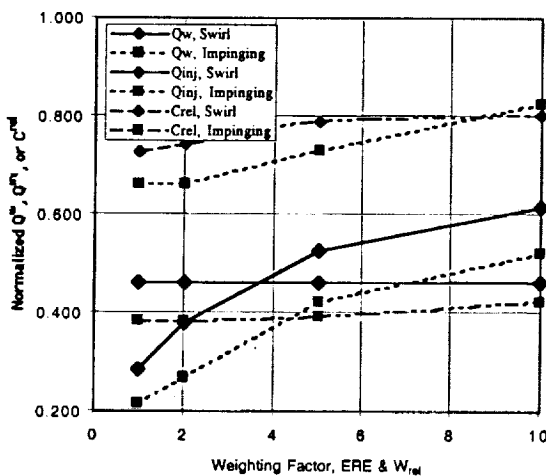
Figure 5. Heat flux and cost trends for swirl and impinging elements.

The impacts on Q_w , Q_{inj} , and W_{rel} which result from increasing the thrust-to-weight ratio are shown in Figure 5. The Q_w for the impinging element increases rapidly, while Q_w for the swirl element is flat. As expected, increasing ERE

imposes a large Q_{inj} penalty on both elements. Also, emphasis on thrust-to-weight results in increased cost for both elements, with the already higher swirl element cost increasing more rapidly than the C_{rel} for the impinging element.

SUMMARY

Both swirl coaxial and F-O-F impinging GO_2/GH_2 injector element designs have been employed to facilitate optimization studies. Starting with propellant pressure drops, combustor length, and full cone swirl angle or impingement half-angle, an empirical design methodology was used to calculate the dependent variables for both element types. The dependent variables were energy release efficiency, chamber wall and injector face heat fluxes, relative chamber weight, and relative injector cost. The response surface methodology was used to fit the results for both elements with quadratic polynomials. Desirability functions were used to create joint response surfaces that were used in the optimization studies.

Three sets of results for both elements were generated to illustrate the capability of *method i* in the context of injector design and optimization. The first set of results started with a design optimized for *ERE* and then added the other four dependent variables to the design one at a time. Most sequential optimal designs were different than previous designs, with the final design being quite different than the initial design. The result showed the importance of including as many variables as possible early in the design. The optimization techniques embodied in *method i* facilitate this early inclusion by allowing efficient management of large amounts of data.

The second set of results focused on the inherent design trade-offs between performance and component life. Different weights were applied to emphasize variables related to performance (*ERE* and W_{rel}). While the thrust to weight ratio was improved, the adverse affect on variables related to component life (Q_w and Q_{inj}) were clearly shown. Conversely, when Q_w and Q_{inj} were emphasized, the toll on the performance variables was clear. These techniques can be used to identify both qualitative trends and to

12

examine the quantitative trade-offs present in this and other design processes.

The third illustration combined results from both elements to show the effects on all dependent variables of increasing the thrust-to-weight ratio. Here, objective assessments can be made on the penalties on Q_w, Q_{inj}, and C_{rel} for an individual element. Also, the relative penalties can be compared for different elements. This ability can provide the injector designer to include margins and robustness in the choice of element type for a particular application.

The flexibility and utility of *method i* have been demonstrated in this effort. Use of *method i* can allow an injector designer to confidently and efficiently manage large amounts of data to conduct a range of design optimization studies. Constraints on independent variables can be modified to allow optimum designs to be sought in specific portions of the parameter space. Also, individual or specific groups of dependent variables can be emphasized to reflect a designer's priorities in the design optimization process.

REFERENCES

1. Personal Communication with Garry Lyles.

2. Rupe, J. H., "An Experimental Correlation of the Nonreactive Properties of Injection Schemes and Combustion Effects in a Liquid Rocket Engine," NASA TR 32-255, 1965.

3. Pieper, J. L., "Oxygen/Hydrocarbon Injector Characterization," PL-TR 91-3029, October, 1991.

4. Nurick, J. H., "DROPMIX - A PC Based Program for Rocket Engine Injector Design," JANNAF Propulsion Conference, Cheyenne, Wyoming, 1990.

5. Dickerson, R., Tate, K., Nurick, W., "Correlation of Spray Injector Parameters with Rocket Engine Performance," AFRPL-TR-68-11, January, 1968.

6. Pavli, A. L., "Design and Evaluation of High Performance Rocket Engine Injectors for Use with Hydrocarbon Fuels," NASA TM 79319, 1979.

7. Tucker, P. K., Shyy, W, Sloan, J. G., "An Integrated Design/Optimization for Rocket Engine Injectors," 34th AIAA/ASME/SAE/ASEE Joint Propulsion Conference and Exhibit, July 13-15, 1998, AIAA 98-3513, Cleveland, OH.

8. Shyy, W, Tucker, P. K. and Vaidyanathan, R., "Response Surface and Neural Network Techniques for Rocket Engine Injector Optimization," 35th AIAA/ASME/SAE/ASEE Joint Propulsion Conference and Exhibit, June 20-23, 1999, AIAA 99-2455, Los Angeles, CA.

9. Calhoon, D., Ito, J. and Kors, D., "Investigation of Gaseous Propellant Combustion and Associated Injector-Chamber Design Guidelines," Aerojet Liquid Rocket Company, NASA CR-121234, Contract NAS3-13379, July 1973.

10. Calhoon, D., Ito, J. and Kors, D., "Handbook for Design of Gaseous Propellant Injectors and Combustion Chambers," NASA CR-121234, Contract NAS3-13379, July 1973

11. Myers, R.H. and Montgomery, D. C., Response Surface Methodology-Process and Product Optimization Using Designed Experiments, John Wiley & Sons, 1995.

12. Gill, G. S., and Nurick, W. H., Liquid Rocket Engine Injectors, NASA SP-8089, March, 1976.

13. Doumas, M. and Laster, R., "Liquid-Film Properties for Centrifugal Spray Nozzles," Chemical Engineering, Vol.49, No. 10, pp. 518-526, October, 1953.

14. Santoro, R. J., "An Experimental Study of Characteristic Combustion-Driven Flow for CFD Validation," Final Report for NASA Contract NAS8-38862, October, 1997.

15. Tucker, P. K., Klem, M. D., Smith, T. D., Farhangi, S., Fisher, S. C., and Santoro, R. J., "Design of Efficient GO_2/GH_2 Injectors: A NASA, Industry and University Effort," AIAA 97-3350, 33rd AIAA/ASME/SAE/ASEE Joint Propulsion Conference, July 6-9, 1997, Seattle, WA.

16. Gill, G. S., and Nurick, W. H., "Liquid Rocket Engine Injectors," NASA SP-8089, March, 1976.

17. SAS Institute Inc. (1995). JMP version 3. Cary, NC.

18. Microsoft Corporation. (1985-1996). Microsoft Excel 97